

Supplementary Information Appendix for

ENDOSOMAL SIGNALING OF DELTA OPIOID RECEPTORS IS AN ENDOGENOUS MECHANISM AND THERAPEUTIC TARGET FOR RELIEF FROM INFLAMMATORY PAIN

Nestor N Jimenez-Vargas¹, Jing Gong², Matthew Wisdom³, Dane D. Jensen^{3,4}, Rocco Latorre³, Alan Hegron³, Shavonne Teng³, Jesse J. DiCello⁵, Pradeep Rajasekhar⁵, Nicholas A. Veldhuis^{5,6}, Simona E. Carbone⁵, Yang Yu¹, Cintya Lopez-Lopez¹, Josue Jaramillo-Polanco¹, Meritxell Canals⁷, David E. Reed¹, Alan E. Lomax¹, Brian L. Schmidt⁴, Kam Leong², Stephen J. Vanner¹, Michelle L Halls⁵, Nigel W. Bunnett^{3*}, Daniel P. Poole^{5,6}

Corresponding Author: Nigel W. Bunnett, B.Sc., Ph.D., Department of Molecular Pathobiology, New York University, 345 East 24th Street, 902A, New York, NY 10010, USA; C: 917-675-0309; E: nwb2@nyu.edu

This PDF file includes:

- Supplementary text
- Figures S1 to S6
- Tables S1 to S2
- Captions to movies S1 to S2
- References for SI reference citations

Other supplementary materials for this manuscript include the following:

- Movies S1 to S2

Supplementary Information Text

Materials and Methods

Materials. SNC80 ((+)-4- [(α R)- α -((2S,5R)-4-allyl-2,5-dimethyl-1-piperazinyl)-3-methoxybenzyl]-N,N-diethylbenzamide), ARM390 (AR-M100390, N,N-diethyl-4-(phenylpiperidin-4-ylidene-methyl)-benzamide), Dyngo4a (Dy4) and PitStop2 (PS2) were from Tocris (Ellisville, MO). Other reagents, including DADLE ([d-Ala 2-d-Leu 5] enkephalin) and DAMGO ([d-Ala 2, N-Me-Phe 4, Gly 5-ol] enkephalin), were from Sigma Aldrich (St Louis, MO) unless stated otherwise.

Mice. C57BL/6 mice (male, 6-10 weeks) were from Charles River Laboratory (Wilmington, MA, USA) and Jackson Laboratory (Bar Harbor, ME, USA). DOPr-eGFP knockin mice (male and female, 6-8 weeks) were from B. Kieffer (McGill) and have been described (1). Mice were maintained in a light (12 h cycle) and temperature (25°C) controlled environment with free access to food and water. Mice were killed by cervical dislocation or anesthetic (isoflurane) overdose and bilateral thoracotomy. Animal ethics committees of Queen's University, Monash University and New York University approved all procedures.

Mouse colon supernatants. To induce chronic colitis, mice were treated for three cycles with 2% DSS in drinking water (each cycle, 5 days DSS and 5 days of normal water). Control mice received normal drinking water. Whole colon was cut into segments (~ 1 mm³) and incubated in RPMI medium (1 mL per cm colon) containing 10% fetal calf serum, penicillin/streptomycin and gentamicin/amphotericin B (95% O₂ 5% CO₂, 24 h, 37°C). Supernatants were stored at -80°C.

Human colon supernatants. Biopsies of mucosa were collected from the descending colon of three patients with active chronic ulcerative colitis and three healthy control patients (SI Appendix, Table S1). The protocol was approved by the Queen's University Human Ethics committee. Tissue supernatants were obtained as described (2).

Dissociation of DRG neurons for electrophysiology. DRG neurons (T9-T13) from C57BL/6 mice were dissociated by incubation with collagenase (1 mg/mL) and dispase (4 mg/mL) for 10 min at 37 °C, and trituration with a fire-polished Pasteur pipette (3). Cells were plated onto glass coverslips coated with laminin (0.017 mg/mL) and poly-D-lysine (2 mg/mL). Neurons were cultured in F12 medium containing 10% fetal calf serum, with penicillin and streptomycin and maintained at 37 °C in a humidified atmosphere of 95% air and 5% CO₂ for 16 h.

Patch clamp recording from DRG neurons. The excitability of small diameter neurons (<30 pF capacitance) was assessed by perforated patch-clamp with amphotericin B (240 µg/mL) in current clamp mode at room temperature (2-5). Only neurons with resting membrane potentials more negative than -40 mV were analyzed. Changes in excitability were quantified by measuring rheobase (minimum input current to elicit action potential). Recordings were made using Axopatch 200B amplifiers, digitized by Digidata 1550B and stored and processed using pClamp 11.03 software (Molecular Devices). The recording chamber was continuously perfused with external solution at 2 mL/min. External solution was (mM): 140 NaCl, 5 KCl, 10 HEPES, 10 D-glucose, 1 MgCl₂, 2 CaCl₂; pH to 7.4 with 3 M NaOH. Pipette solution was (mM): 110 K-gluconate, 30 KCl, 10 HEPES, 1 MgCl₂, 2 CaCl₂; pH 7.25 with 1 M KOH. To study the effects of endogenous opioids released from inflamed colon, neurons were pre-incubated for 60 min with cDSS or HC supernatant (50 µL supernatant, 950 µL of F12 medium, filtered) or with cUC or HC supernatants (200 µL supernatant, 500 µL of F12 medium, filtered), and were then washed with F12 medium. To evaluate the effects of selective OPr agonists, neurons were pre-incubated for 15 min with DADLE (10 nM), SNC80 (10 nM), ARM390 (100 nM), DAMGO (10 nM) or vehicle (control) and were then washed. Some neurons were also incubated overnight (12-16 h) with DADLE (100 nM) or ARM390 (300 nM) and were washed. Rheobase was measured at T=0 min or T=30 min after washing. To evaluate the participation of specific OPrs, neurons were pre-treated with the DOPr antagonist SDM25N (100 nM, 30 min) or the MOPr antagonist CTOP (100 nM, 30 min) before supernatant challenge. To investigate the role of endocytosis, neurons were pre-treated with Dy4 (30 µM, 30 min) or PS2 (15 µM, 30 min) before supernatant or OPr agonists. To identify the signaling pathway responsible for altered excitability, neurons were pre-treated with inhibitors of PKC (GF109203X, 1 µM) or MEK1 PD98059 (50 µM) for 30 min before OPr agonists.

Extracellular recording from colonic afferents. The distal colon with attached mesentery containing the inferior mesenteric ganglia was excised and mounted in an organ bath continuously superfused with gassed (5% CO₂, 95% O₂) Krebs buffer (mM: NaCl, 118.4;

NaHCO₃, 24.9; MgSO₄, 1.2; KH₂PO₄, 1.2; glucose, 11.7; CaCl₂, 1.9) at 34°C (3). Preparations were opened longitudinally along the mesentery border and pinned flat with mucosal side up. The lumbar splanchnic nerve was identified in the neurovascular bundle, teased into 5-6 fibers, and individually drawn into a glass suction electrode attached to a Neurolog headstage (NL100, Digitimer, Welwyn Garden City, UK). Afferent nerve signals were amplified (NL104), filtered (NL125 band pass filter), and recorded on a computer with Micro 1401 interface and Spike 2 software (Version 7, Cambridge Electronic Design, Cambridge, UK). Krebs contained the L-type calcium channel blocker nifedipine (3 μM) and the muscarinic acetylcholine receptor antagonist atropine (5 μM) to suppress smooth muscle activity, as well as the cyclooxygenase inhibitor indomethacin (3 μM) to suppress potential inhibitory actions of endogenous prostaglandins. Receptive fields were identified by systematically stroking the mucosal surface and the mesenteric attachment with a brush (6, 7). Once identified, receptive fields were tested with 3 distinct mechanical stimuli to allow classification: probing (von Frey filament, VFF, 1 g), mucosal stroking (0.4 g) and stretch. Vascular afferents that only respond to probing of the gut wall or the mesenteric attachment were included. After 30 min equilibration, control probing responses of each unit were examined by probing 3 times, each for 3 s (VFF 1 g). OPr agonists (SNC80, ARM390, DAMGO; 100 nM) were superfused into the organ bath for 15 min. Tissue was washed to remove agonists, and afferent responses to VFF probing were re-assessed every 15 min for 60 min. To examine the contribution of endocytosis, colonic segments were pre-incubated for 15 min with PS2 (50 μM) before challenge with SNC80. PS2 was included throughout the experiment. Single unit activity was analyzed offline using the spike sorting function of Spike 2 to discriminate the afferent nerve activity of individual units. The afferent response to probing was assessed as average firing frequency during a 3-s period using a custom-made script in Spike2. Baseline was assessed as average firing frequency during a 120-s period.

cDNAs. Human DOPr (untagged), DOPr with N-terminal extracellular HA epitope (HA-DOPr), Gβ1 (untagged), HA-tagged wild-type and K44E dominant negative mutant dynamin I cDNAs have been described (8, 9). Gα₁-Rluc8, Gα₂-Rluc8, Gα₃-Rluc8, Gα_o-Rluc8, Gα_s-Rluc8, Gα_q-Rluc8, and Gγ2-Venus were from C. Gales (Institut des Maladies Métaboliques et Cardiovasculaires, Université Toulouse, France) (10). βARR1-YFP and βARR2-YFP were from M. Caron (Duke University). KRas-Venus, HRas-Venus, Rab5a-Venus, Rab7a-Venus and Rab11a-Venus were from N. A. Lambert (Augusta University) (11). Mini-G proteins coupled to Venus were from N. A. Lambert, (Augusta University) (12). Constructs were modified to replace Venus with Rluc8. RGFP-CAAX, RGFP-Rab5a and Rluc2-βARR2 were from M. Bouvier (Université de Montréal) (13). βARR1 conjugated at the C-terminus with the helper peptide Sp1 was from J. A. Javitch (Columbia University). The plasmid for expression of human DOPr was from cdna.org (#OPRD10TN00, Bloomsburg, PA). The coding sequence for DOPr was cloned into pcDNA3.1 with a C-terminal Rluc8 tag using NEBuilder HiFi DNA Assembly Cloning from New England BioLabs (E5520S, Ipswich, MA). DOPr-Rluc was from G. Pineyro (Université de Montréal, Québec, Canada) and FRET sensors cytoEKAR GFP/RFP (Addgene plasmid 18680), cytoEKAR Cerulean/Venus (Addgene plasmid 18679), nucEKAR GFP/RFP (Addgene plasmid 18681) and nucEKAR Cerulean/Venus (Addgene plasmid 18681) were from K. Svodoba (Howard Hughes Medical Institute, Ashburn, VA, USA) (14), and cytoCKAR (Addgene plasmid 14870) and pmCKAR (Addgene plasmid 14862) were from A. Newton (University of California at San Diego, CA, USA) (15). βARR1/2 and scrambled siRNA have been described (16, 17).

Cell culture and transfection. For BRET assays of G protein activation, HEK293 cells were seeded in 10 cm dishes in Dulbecco's Modified Eagle Medium (DMEM) with 10% v/v FBS. Upon reaching 50% confluence 24 h post seeding, cells were co-transfected with a total of 5 µg of DOPr: Gα-Rluc8: Gβ1: Gγ2-Venus at a ratio of 1.2: 0.3: 1.2: 2.4, respectively. For the βARR1/2 and plasma membrane/endosomal trafficking BRET assays, HEK293 cells were co-transfected with DOPr-Rluc (1 µg) and βARR1-YFP, KRas-Venus, HRas-Venus, Rab5a-Venus, Rab7a-Venus or Rab11a-Venus (4 µg). After 24 h, cells were plated onto poly-D-lysine-coated white 96-well plates and cultured for a further 24 h prior to BRET assays. For ebBRET assays of trafficking of mini-G proteins to the plasma membrane or early endosomes, HEK293T cells were transfected using JetPEI (Polyplus Transfection, France) with DOPr (0.3 µg) and Rluc8-mGα_{si/o/s/sq} (12, 18) (0.3 µg) and either *Renilla* (R) GFP-CAAX (prenylation CAAX box of KRas) (13) (0.4 µg) for cell surface activation or tRGFP-Rab5a (0.4 µg) for activation in early endosomes. For ebBRET assays of recruitment of βARRs to the plasma membrane or early endosomes, HEK293T cells were transfected with JetPEI with DOPr (0.3 µg) and Rluc2-βARR2 (13) or Rluc8-βARR1 conjugated at the C-terminus with the helper peptide Sp1 (19) (0.1 µg), and RGFP-CAAX (0.4 µg) for plasma membrane recruitment or tRGFP-Rab5a (0.4 µg) for early endosome recruitment. For the FRET assays of compartmentalized signaling, HEK293 cells were seeded into poly-D-lysine-coated black, optically clear 96-well plates. Upon reaching 50-70% confluence 24 h post seeding, HEK293 cells were transfected with DOPr (untagged) (55 ng/well) and FRET biosensors (40 ng/well). An additional 50 ng/well of either the wild-type or K44E dynamin I was transfected for the endocytic inhibitory experiments. βARR1/2 knockdown has been described (16, 17). After 24 h, the cells were subjected to partial serum restriction (0.5% v/v FBS DMEM) overnight prior to FRET assays.

Dissociation of DRG neurons for DOPr trafficking and signaling assays. DRG (all levels) from DOPr-eGFP mice were digested in Ca²⁺/Mg²⁺-free Hank's Balanced Salt Solution (CMF-HBSS) containing collagenase Type IV (2 mg/mL), dispase II (2 mg/mL) and DNase (0.1 mg/mL) (30 min, 37°C) (20). DRG were triturated using large, medium and small fire-polished pipettes 30, 15 and 10 min post-digestion. Neurons were dispersed in 5 mL of DMEM and centrifuged (500 x g, 5 min). The supernatant was aspirated and the wash was repeated to remove residual enzymes. For FRET assays, neurons were nucleofected with 600 ng of the FRET biosensors using a Lonza 4D-Nucleofector™ system and P3 Primary Cell 4D-Nucleofector™X Kit, according to the manufacturer's instructions. Neurons were resuspended in DMEM containing 10% v/v FBS, 1% v/v antibiotic/antimycotic solution (P/S/F) and 1% v/v N1 medium supplement prior to seeding into poly-L-lysine- and laminin-coated half area black, optically clear 96-well plate. After 24 h, the neurons were subjected to partial serum restriction (DMEM with 0.5% v/v FBS, 1% v/v P/S/F, 1% v/v N1) overnight prior to FRET assessment.

BRET assays of G protein activation and DOPr and βARR trafficking. HEK293 cells were equilibrated in HBSS at 37°C for 30 min. Coelenterazine h (3 µM) was added 15 min prior to BRET detection. Cells were challenged with graded concentrations of SNC80, DADLE or ARM390. BRET was measured for 3 min before and 15-25 min after agonist stimulation using a PHERAstar microplate reader (BMG LabTech, Offenburg, Germany) (16, 17). For the plasma membrane/endosomal trafficking assays, BRET was measured for 10-60 min after agonist stimulation. The BRET signal was calculated as a ratio of the Venus or YFP emission (530-535 nm) over the Rluc8 or Rluc emission (430-475 nm).

BRET assays of mini-G protein and β ARR recruitment to the plasma membrane and early endosomes. HEK293 cells were washed with Dulbecco's phosphate-buffered saline, and then Tyrode's buffer was added. After the addition of Prolume Purple Coelenterazine (2.5 μ M; NanoLight Technology), the cells were incubated for 5 min at 37°C. EbbRET was recorded for 22.5 min in a Synergy Neo2 Microplate reader (BioTek) (acceptor filter: 515 \pm 30 nm; donor filter: 410 \pm 80 nm). Cells were challenged with SNC80, DADLE or ARM390 (100 nM) after 2.5 min. In some experiments, cells were pretreated with pertussis toxin (100 ng/ml, 24 h). Δ -BRET represents the ebbRET signal in the presence of agonist subtracted by the ebbRET signal in the presence of vehicle.

FRET assays of compartmentalized signaling. HEK293 cells and DRG neurons were equilibrated in HBSS at 37°C. Images were captured at 1 min intervals using a GE Healthcare INCell 2000 Analyzer with a Nikon Plan Fluor ELWD 40x (NA 0.6) objective and FRET module (Little Chalfont, UK) as described (17, 20). For the GFP/RFP ERK biosensors, cells were sequentially excited using a light source with a FITC filter (490/20) and emission was measured using dsRed (605/52) and FITC (525/36) filters in addition to a polychroic filter (Quad 4) optimized for the FITC/dsRed filter pair. For the Cerulean/Venus ERK biosensors and the PKC biosensors, cells were sequentially excited using a light source with a CFP filter (430/24) and emission was measured using YFP (535/30) and CFP (470/24) filters in addition to a polychroic filter (Quad3) optimized for the CFP/YFP filter pair. GFP/RFP ERK biosensors were used in HEK293 cells whereas the Cerulean/Venus ERK biosensors were used for the GFP-dynamin and DRG experiments to avoid GFP interference. Cells were challenged with SNC80, DADLE or ARM390 (100 nM). Baseline images were taken for 4 min prior to stimulation. Upon addition of ligands, images of the stimulated cells were taken for 20 min. Cells were then stimulated with positive control compounds (200 nM phorbol 12,13 dibutyrate (PDBu) for ERK biosensors, or 200 nM PDBu with phosphatase inhibitor cocktail for PKC biosensors) for 10 min to generate maximal responses. HEK293 cells and DRG neurons were pre-treated with the dynamin inhibitor Dy4 (50 μ M) (Abcam, Cambridge, MA), the clathrin inhibitor PS2 or inactive PS2 (30 μ M) (Abcam, Cambridge, MA) or vehicle (1% DMSO) for 30 min and inclusion throughout. FRET images were automatically collated and aligned in the order of baseline, stimulated and positively stimulated prior to manual selection with the aid of scripts as described. The baseline subtracted ratio relative to positive control (F/F_{\max}) for each cell was then graphed if the selection criteria of having greater than 5% change in emission ratio relative to baseline (F/F_0) post positive control stimulation was met.

Immunofluorescence. After FRET imaging, DRG were fixed with 4% paraformaldehyde (PFA) (20 min at 4°C). Neurons were blocked with 5% normal horse serum (NHS) and 0.1% saponin in PBS, and incubated with rabbit anti-GFP (#A11122, ThermoFisher Scientific; 1:1000) and mouse anti-NeuN (clone A60, Merck Millipore, Bedford, MA; 1:200) (overnight, 4°C). Neurons were washed with PBS and incubated with donkey anti-mouse Alexa Fluor 647 (1:500) and donkey anti-rabbit Alexa Fluor 488 (1:1000) (ThermoFisher Scientific) (2 h, RT). Images were captured using the INCell 2000 Analyzer with Cy5 (645/30) and FITC (490/20) as the excitation filters and Cy5 (705/72) and FITC (525/36) as the emission filters in addition to a polychroic filter (Quad 4). FRET was only analyzed in neurons expressing DOPr-eGFP.

DOPr-eGFP trafficking in DRG neurons. DRG (all levels) were collected from DOPr-eGFP mice. Neurons were dispersed and plated on poly-l-lysine/laminin-coated glass coverslips. After 48 h, neurons were exposed to vehicle, DADLE (1 μ M), DADLE-LipoMSN-Alexa647 (1 μ M DADLE, 10 μ g/mL LipoMSN) or LipoMSN-Alexa647 (10 μ g/mL LipoMSN, control) (30 or 60 min, 37°C in serum-free DMEM). In some experiments, neurons were preincubated with Dy4 (30 μ M) or PS2 (15 μ M) (30 min preincubation, inclusion throughout). Neurons were fixed in 4% PFA for 20 min on ice, and then blocked 5% NHS, 0.1% Triton X-100 in PBS containing 0.1% sodium azide (1 h, RT). Neurons were incubated with rabbit anti-GFP (#A11122, ThermoFisher Scientific; 1:1000) and mouse anti-HuC/HuD (# A-21271, 16A11, ThermoFisher Scientific; 1:1000) (overnight, 4°C). Neurons were washed in PBS and incubated with donkey anti-rabbit A488 and donkey anti-mouse A568 (ThermoFisher Scientific; 1:500) (1 h, RT in PBS). Neurons were imaged using a Leica TCS SP8 confocal microscope (40x objective, 1024x1024 and 2048x2048 resolution, 16-bit depth).

MSN Synthesis. MSNs were prepared as described (21).

Sodium diselenide. Sodium diselenide was prepared by reaction of selenium powder and sodium borohydride in water as described. Sodium borohydride 0.15 g (4.0 mmol) was dissolved in 2 mL of deionized water and mixed with selenium powder 0.32 g (2.0 mmol). The selenium was dissolved, generating hydrogen gas and resulting in a colorless solution within ~5 min. The flask was sealed and the solution was heated to 70°C for 20 min, resulting in a dark red solution. A solution of benzyl bromide 0.68 g (4.0 mmol) in 5 mL refined tetrahydrofuran (THF) was injected into the flask under argon gas. The reaction proceeded at 50°C for 12 h, the product was extracted with CH₂Cl₂ and dried under anhydrous MgSO₄. Evaporation and vacuum drying formed dibenzylidiselinide as a yellow solid. Bibenzylidiselinide was then dissolved in 5 mL THF and added into a 2 mL solution of 0.15 g sodium borohydride. After stirring for 10 min, the solution became colorless and 1.0 g (4 mmol) 11-bromoundecanol in 5 mL THF solution was added. The flask was incubated at 50°C overnight, and the reaction mixture was then extracted with CH₂Cl₂, desiccated by MgSO₄ and concentrated. The crude product was purified using column chromatography by 2 elution steps with CH₂Cl₂ and then diethyl ether. A white powder, 11-(benzylselanyl)undecan-1-ol, was obtained (yield 70%).

Bis[3-(triethoxysilyl)propyl]diselenide. Bis[3-(triethoxysilyl)propyl]diselenide (BTESePD) was prepared by the reaction of γ -chloropropyl trimethoxysilane with freshly prepared sodium diselenide as described. γ -chloropropyl trimethoxysilane (10 g) was added into 30 mL of sodium diselenide stock solution and stirred at room temperature overnight. Ice water was used to quench the reaction. The mixture was extracted with dichloromethane and the organic layer was dried with anhydrous sodium sulfate. The crude product was purified by silica-gel column chromatography (PE:DCM, 10:1-1:1) to obtain the product, appearing as a dark yellow liquid (1.8 g, yield 18%).

Biodegradable MSNs. Biodegradable MSNs were synthesized through a modified sol-gel method using cetyltrimethylammonium tosylate (CTAT) as a template, TEOS and bis-silylated precursors with diselenide-bridged groups as co-silica sources as described. To prepare diselenide-bridged MSNs, 0.6 g CTAT, 0.15 g triethanolamine (TEAH₃) and 40 mL deionized water were stirred at 80°C for 30 min. A solution of 4.0 g TEOS and 1.0 g bis[3-(triethoxysilyl)propyl]diselenide (BTESePD) was added dropwise to the surfactant solution and mixed at 80°C for 4 h. The products were collected by centrifugation, washed three times with ethanol, and then refluxed in an ethanol solution of NH₄NO₃ (1% w/v) for 12 h. MSNs were collected, washed, and dried for subsequent experiments.

DOPr-targeted liposome synthesis

Cationic liposome assembly. Lipid was formulated into liposomes for all delivery applications as described (22). 1,2-Dioleoyl-3-trimethylammonium propane (DOTAP) was mixed with cholesterol, dioleoylphosphatidylethanolamine (DOPE), and 1,2-distearoyl-sn-glycero-3-phosphoethanolamine-N-[amino(polyethylene glycol)-2000] (DSPE-PEG2000-maleimide) (Avanti Polar Lipids) at a molar ratio of 65:30:3.75:12.5. Briefly, DOTAP, cholesterol, DOPE and half of the DSPE-PEG were mixed in a chloroform solution. The organic solvent was evaporated under vacuum and further dried over night to form a thin layer film. The lipid film was hydrated using a mixed solution of ethanol/sodium acetate buffer (200 mM, pH 5.2, vol:vol, 9:1). The solution was added dropwise to an aqueous solution containing the rest of the DSPE-PEG, and the resulting solution was incubated at 37°C for 30 min before dialysis against water in 3500 molecular weight cut-off cassettes.

Liposome conjugation to DADLE. DADLE was covalently tethered to the maleimide end of the DSPE-PEG-2000-maleimide inserted into the liposome by a thioether bond (23). To ensure correct orientation of the DADLE, a C-terminal cysteine residue was added to the DADLE peptide before reacting the DADLE with the formulated liposome. DADLE-cysteine and liposomes were mixed in a 1:1 molar ratio in 20 mM MES, 20 mM HEPES, pH 6.5 buffer under inert N₂ conditions (4°C, overnight, dark, gentle stirring). The reaction was dialyzed against water in 3500 molecular weight cut-off cassettes.

Cargo loading and liposome coating

MSN core-loading. DADLE, Alexa647-DADLE or Alexa647 (10 mM) was added to aqueous MSN (1 mg/mL) in 1:10 ratio (wt:wt). The solution was shaken at 500 rpm at 4°C for 30 min. To remove excess DADLE, the solution was centrifuged (10,000 g, 4°C, 10 min) and supernatant was discarded. The pellets of MSN-DADLE, MSN-Alexa647-DADLE or MSN-Alexa647 were resuspended by pipetting and sonication (2 min).

Liposome coating. Liposomes and MSNs were combined in aqueous solution in a 1:1 ratio (wt:wt). The solution was shaken at 500 rpm at 4°C for 30 min. To remove excess liposome, the solution was centrifuged (10,000 g, 4°C, 10 min) and supernatant was discarded. The pellet of LipoMSN was resuspended by pipetting and sonication (2 min).

LipoMSN-SDM25N synthesis

Cationic liposome assembly. Liposomes were formulated as described above with DOTAP, cholesterol, DOPE, and DSPE-PEG2000 at a molar ratio of 65: 30: 3.5: 17.5.

MSN core-loading. MSNs (1 mg/mL) were loaded with SDM25N (10 mM) in 1:10 ratio (wt:wt) as described above.

Liposome coating. MSN-SDM25N were coated with liposomes as described above.

Physicochemical characterization of LipoMSNs

Transmission electron microscopy. The morphology of the nanoparticles was characterized using a JEM-2100F transmission electron microscope (TEM, JEOL, Ltd., Japan).

Size and charge. The hydrodynamic diameter and zeta potential of the nanoparticles in water or PBS were determined using a Nano-ZS 90 Nanosizer (Malvern Instruments Ltd., Worcestershire, UK).

Drug-loading efficiency. DADLE and SDM25N loading of MSNs was measured by absorbance using a Fluostar Optima plate reader (BMG Labtech, Ortenberg, Germany). Supernatant was collected after loading the MSN core with DADLE or SDM25N and the concentration was measured at 280 nm or 290 nm with a standard curve of DADLE or SDM25N, respectively. The supernatant concentration was used to calculate the unloaded fraction of peptide, yielding the remaining as the loaded fraction.

pH- and glutathione-sensitive cargo release. To determine the pH or redox-sensitive cargo release from LipoMSN, Alexa Fluor 647-tagged DADLE (DADLE-647) was loaded into the MSN and the fraction loaded was calculated by supernatant measurement. For pH-sensitive release, DADLE-647-MSNs were incubated in PBS (pH 7.2) or sodium acetate buffer (pH 5.2), or with and without 10 mM glutathione. Supernatant was collected by centrifugation (10,000 g, 12 min) at 30 min, 1 h, 2 h, 4 h and 24 h time points. DADLE-647 released into the supernatant was determined by measurement of fluorescence using a Fluostar Optima plate reader (BMG Labtech, Ortenberg, Germany), and total DADLE-647 released in each time frame was calculated. Standard curves of DADLE-647 were generated in both buffers. For redox-sensitive release, DADLE-647-MSNs were incubated in an aqueous solution with or without 10 mM glutathione. Release of DADLE-647 was measured as described, using standard curves in aqueous solution with or without glutathione.

Cellular targeting of LipoMSNs. The MSN core of DADLE-LipoMSNs and LipoMSNs was loaded with Alexa Fluor 647. HEK293T cells were transfected using polyethylenimine with 5 μ g cDNA encoding human HA-DOPr; untransfected cells were used as controls. Cells were plated 24 h after transfection. For flow cytometry experiments, cells were seeded at 100,000 cells per well in a 24-well plate and cultured overnight. Cells were incubated with DADLE-LipoMSN-Alexa647 or LipoMSN-Alexa647 (40 μ g/mL) in Opti-MEM for 0-4 h. Uptake of nanoparticles was quantified by flow cytometry (LSRFortessa Cell Analyzer, BD Biosciences, Mississauga, Canada). In some experiments, cells were preincubated with Dy4, PS2 or inactive analogs (10 μ g/mL) for 30 min before addition of nanoparticles. For imaging studies, cells were seeded at 30,000 cells onto poly-D-lysine-coated glass coverslips and were infected with Rab5a-GFP (CellLight Early Endosome-GFP, ThermoFisher Scientific; 3 μ L/10,000 cells). After 24 h, cells were pre-incubated with rat anti-HA (Roche clone 3F10; 1:500) in HBSS (30 min, 4°C). Cells were washed and then incubated in HBSS with DADLE-LipoMSN-Alexa647 (20 μ M DADLE, 200 μ g/mL LipoMSN, 4°C, 0-30 min) or LipoMSN-Alexa647 (200 μ g/mL LipoMSN, 4°C, 0-120 min). Cells were fixed in 4% PFA (20 min, 4°C), and blocked in PBS containing 3% NHS, 0.3 % saponin and 0.1% sodium azide (1 h, RT). Cells were incubated with goat anti-rat Alexa Fluor 568 (ThermoFisher Scientific; 1:1000) (1h, RT) and then with DAPI (10 μ g/ μ L, 5 mins, RT). Cells were imaged by confocal microscopy as described above.

Live cell imaging of LipoMSN uptake. HEK293 cells expressing HA-DOPr were seeded on poly-D-lysine coated 35 mm glass bottom dishes (30,000 cells/dish, MatTek) and transduced with the Rab5a-GFP. After 48 h, cells were washed and equilibrated in HBSS (30 min, RT). Images were collected every 15 s for 40 min on a Leica SP8 confocal microscope with a 63x (NA 1.4) objective. After recording baseline for 1 min, cells were challenged with LipoMSN-Alexa647 (200 μ g/mL LipoMSN, control) or DADLE-LipoMSN-Alexa647 (20 μ M DADLE, 200 μ g/mL LipoMSN). Image sequences were processed in ImageJ and videos were rendered in Adobe After Effects.

DADLE-LipoMSN-DADLE and DOPr signaling

cAMP assays. HEK293 cells were co-transfected with 1 µg DOPr and 4 µg CAMYEL cDNA. Cells were plated and BRET was measured after 48 h, as described above. Cells were challenged with forskolin (10 µM, 5 min) to induce cAMP production and were then exposed to DOPr agonists.

βARR1 recruitment. HEK293 cells were co-transfected with 1 µg DOPr-Rluc8, 1 µg GRK2 and 3 µg βARR1-YFP cDNA. Cells were plated and BRET was measured after 48 h, as described above.

Nuclear ERK assays. HEK293 cells were co-transfected with 1 µg DOPr and 4 µg NucEKAR nuclear ERK FRET biosensor. Cells were plated and FRET was measured after 48 h, as described above. Cells were challenged with PDBu (1 µM) or DOPr agonists. FRET ratios were normalized to baseline and to the vehicle control.

Drug treatments. Cells were challenged with DADLE (100 nM), DADLE-LipoMSN (20 µM DADLE, 200 µg/mL LipoMSN), DADLE-LipoMSN-DADLE (20 µM DADLE, 160 µg/mL LipoMSN), LipoMSN (200 µg/mL, control), or vehicle.

DADLE-LipoMSN-DADLE and electrophysiology

Nociceptor excitability. Rheobase was measured at 0, 90, 120 or 180 min after exposure to nanoparticles and washing, as described above. To evaluate the contribution of endocytosis, neurons were pre-incubated with PS2 (15 µM, 30 min and inclusion throughout).

Colonic afferent activity. Colonic afferent responses (1 g VFF) were assessed at 0, 60 and 120 min after exposure to nanoparticles and washing, as described above. To evaluate the contribution of endocytosis, colon preparations were preincubated with PS2 (50 µM, 15 min and inclusion throughout).

Drug treatments. DRG neurons were preincubated with DADLE (100 nM), DADLE-LipoMSN (100 nM DADLE, 1 µg/mL LipoMSN), DADLE-LipoMSN-DADLE (100 nM DADLE, 0.8 µg/mL LipoMSN), LipoMSN (1 µg/mL, control) or vehicle (control) for 30 min and then washed before measurement of rheobase. Colon preparations were preincubated with DADLE-LipoMSN-DADLE (100 nM DADLE, 0.8 µg/mL LipoMSN) for 30 min and then washed before recording colonic afferent activity.

LipoMSN-SDM25N and electrophysiology

Nociceptor excitability. Rheobase was measured at 0 or 30 min after exposure to nanoparticles and washing, as described above.

Drug treatments. DRG neurons were preincubated with LipoMSN-SDM25N (100 nM SDM25N, 100 µg/ml LipoMSN) or LipoMSN (100 µg/ml, control) for 120 min and then washed three times. Neurons were exposed to DADLE (10 nM, 15 min and washed. Rheobase was measured 0 or 30 min after washing.

DADLE-LipoMSN-DADLE and inflammatory pain. The investigator was blinded to the treatments. Mice were randomly assigned to treatments (www.randomization.org). Nociception was assessed from 8 am to 1 pm. Mice were acclimatized to the investigator, room and restraint apparatus for 2 h/day on 2 successive days before experiments. Complete Freund's Adjuvant (CFA, 0.5 mg/mL) was administered by intraplantar injection (10 µL) into the left hindpaw of sedated mice (4% isoflurane). Drugs were administered by intrathecal (i.t.) injection 48 h after

CFA, which is the peak of inflammation in this model of inflammatory pain. DADLE (100 nM), DADLE-LipoMSN-DADLE (100 nM DADLE, 0.8 µg/mL LipoMSN), LipoMSN (1 µg/mL LipoMSN, control) or vehicle (control) was injected intrathecally (5 µL) to sedated mice (4% isoflurane). To assess mechanical hyperalgesia, mice were placed in individual plexiglass boxes on a mesh stand. Paw withdrawal in response to stimulation of the plantar surface of the hind paw with graded VFF was determined using the “up-and-down” paradigm (17, 24). VFF withdrawal thresholds were measured in triplicate to establish a baseline for each mouse on 2 consecutive days before the experiments. Withdrawal thresholds were measured at 1 h intervals for 7 h after i.t. drug administration. Results were normalized to the baseline withdrawal thresholds obtained during the 2 consecutive days of baseline and are expressed as a percentage of baseline.

Statistics. Studies *in vitro* and using cell lines were replicated in at least three independent experiments (N), with triplicate observations in each experiment. For electrophysiological and behavioral studies, the number of replicates (N) was determined from published studies using similar approaches. All results were included and outliers were not excluded. Results were analyzed and graphs prepared using Prism 8 (GraphPad, San Diego, CA). Results are expressed as mean±SEM. Statistical significance was assessed using t-tests or 1-way or 2-way ANOVA with Tukey’s or Sidak’s *post hoc* test (SI Appendix, Table S2).

Supplementary Figures

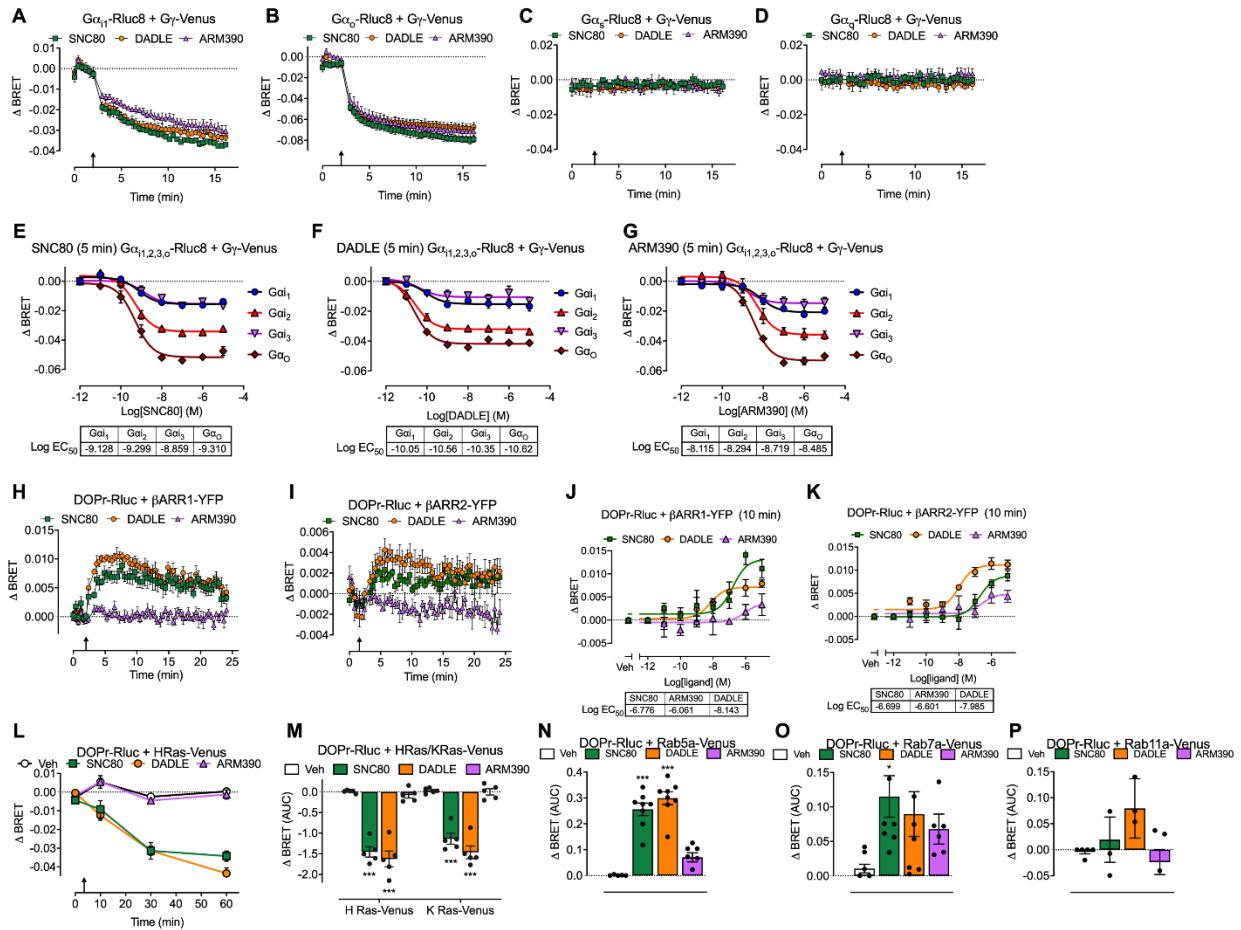


Fig. S1. DOPr signaling and trafficking in HEK293 cells. FRET and BRET biosensors were coexpressed with DOPr in HEK293 cells. **A-D.** Time course of effects of SNC80, DADLE and ARM390 (all 100 nM, arrow) on BRET between $G\alpha_{i1}$ -Rluc8 (**A**), $G\alpha_o$ -Rluc8 (**B**), $G\alpha_s$ -Rluc8 (**C**) or $G\alpha_q$ -Rluc8 (**D**) and $G\gamma$ -Venus. **E-G.** Effects of graded concentrations of SNC80 (**E**), DADLE (**F**) and ARM390 (**G**) on BRET between $G\alpha_{i1,2,3,o}$ -Rluc8 isoforms or $G\alpha_o$ -Rluc8 and $G\gamma$ -Venus. BRET was measured at 5 min after agonist addition. Boxes show Log EC₅₀ values. **H, I.** Time course of effects of SNC80, DADLE and ARM390 (all 100 nM, arrow) on BRET between DOPr-Rluc and β ARR1-YFP (**H**) or β ARR2-YFP (**I**). **J, K.** Effects of graded concentrations of SNC80, DADLE and ARM390 on BRET between DOPr-Rluc and β ARR1-YFP (**J**) or β ARR2-YFP (**K**). BRET was measured at 10 min after agonist addition. Boxes show log EC₅₀ values. **L-K.** Effects of SNC80, DADLE and ARM390 (all 100 nM, arrow) on BRET between DOPr-Rluc and the plasma membrane proteins HRas-Venus (**L, M**) and KRas-Venus (**M**), and the endosomal proteins Rab5a-Venus (**N**, early endosomes), Rab7a-Venus (**O**, late endosomes), and Rab11a-Venus (**P**, recycling endosomes). **L.** Time course. **M-P.** Area under curve (AUC) of 60 min time course. Data points show results of independent experiments. N=3 (**A-G**) or 3-8 (**H-K**) independent experiments (mean \pm SEM). * P <0.05, *** P <0.001, 1-way ANOVA, Tukey's test.

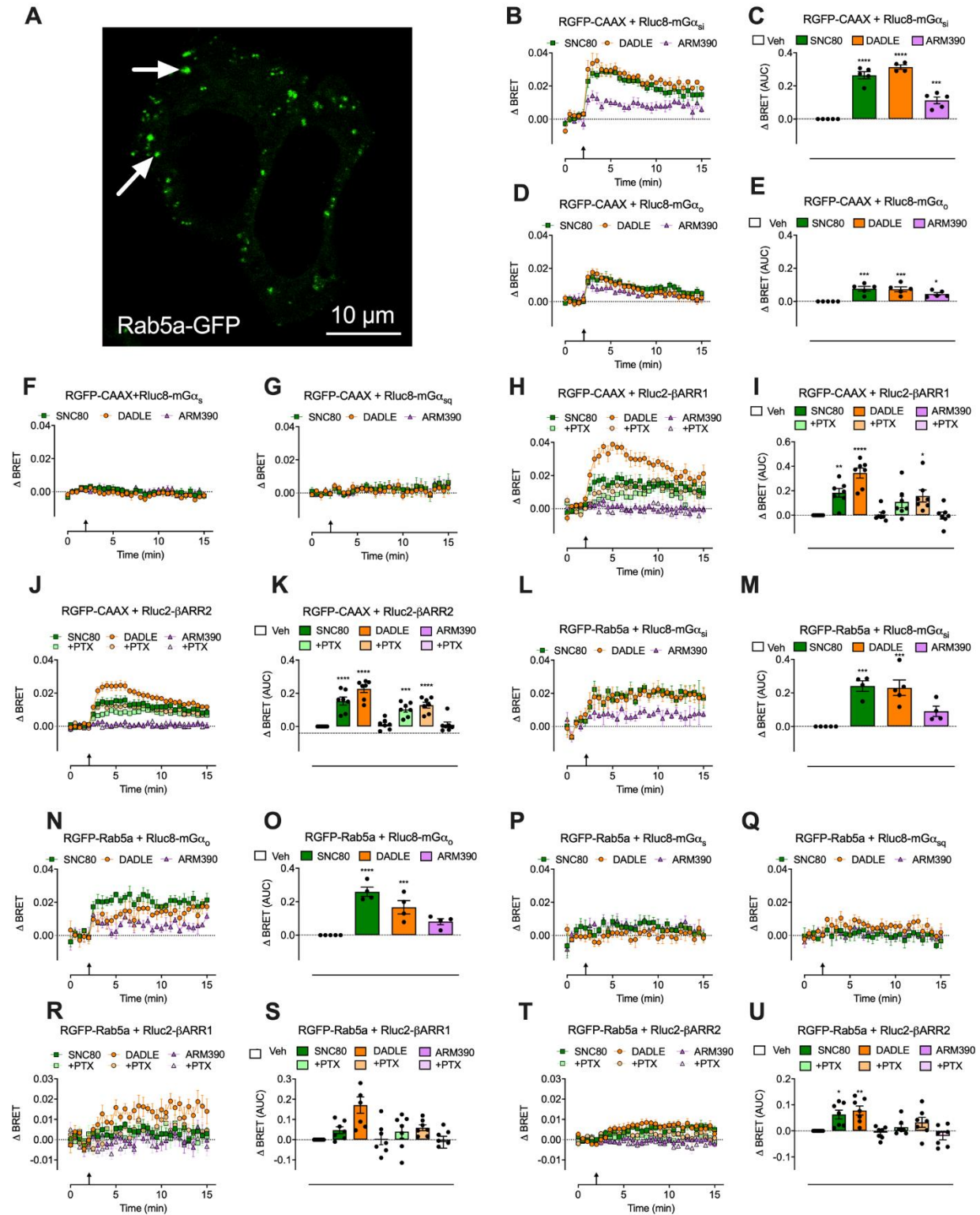


Fig. S2. Activation of G proteins and β ARRs at the plasma membrane and in early endosomes of HEK293 cells. **A.** Localization of Rab5a-GFP in endosomes (arrows). **B-K.** EbBRET for Rluc8-miniG $\alpha_{si/o/s/sq}$ proteins or Rluc2- β ARR1/2 and plasma membrane RGFP-CAAX. **B, D, F, G, H, J, L** show time courses. **C, E, I, K** show the area under curve over 15

min (AUC). **L-U**. EbbRET for Rluc8-mG $\alpha_{si/o/s/sq}$ proteins or Rluc2- β ARR1/2 and early endosomal tdRGFP-Rab5a. **L, N, P, Q, R, T** show time courses. **M, O, S, U** show area under curve over 15 min. Effects of pertussis toxin (PTX) are show in **H-K** and **R-U**. N=5 independent experiments (mean \pm SEM). * P <0.05, ** P <0.01, *** P <0.001, 1-way ANOVA, Tukey's test.

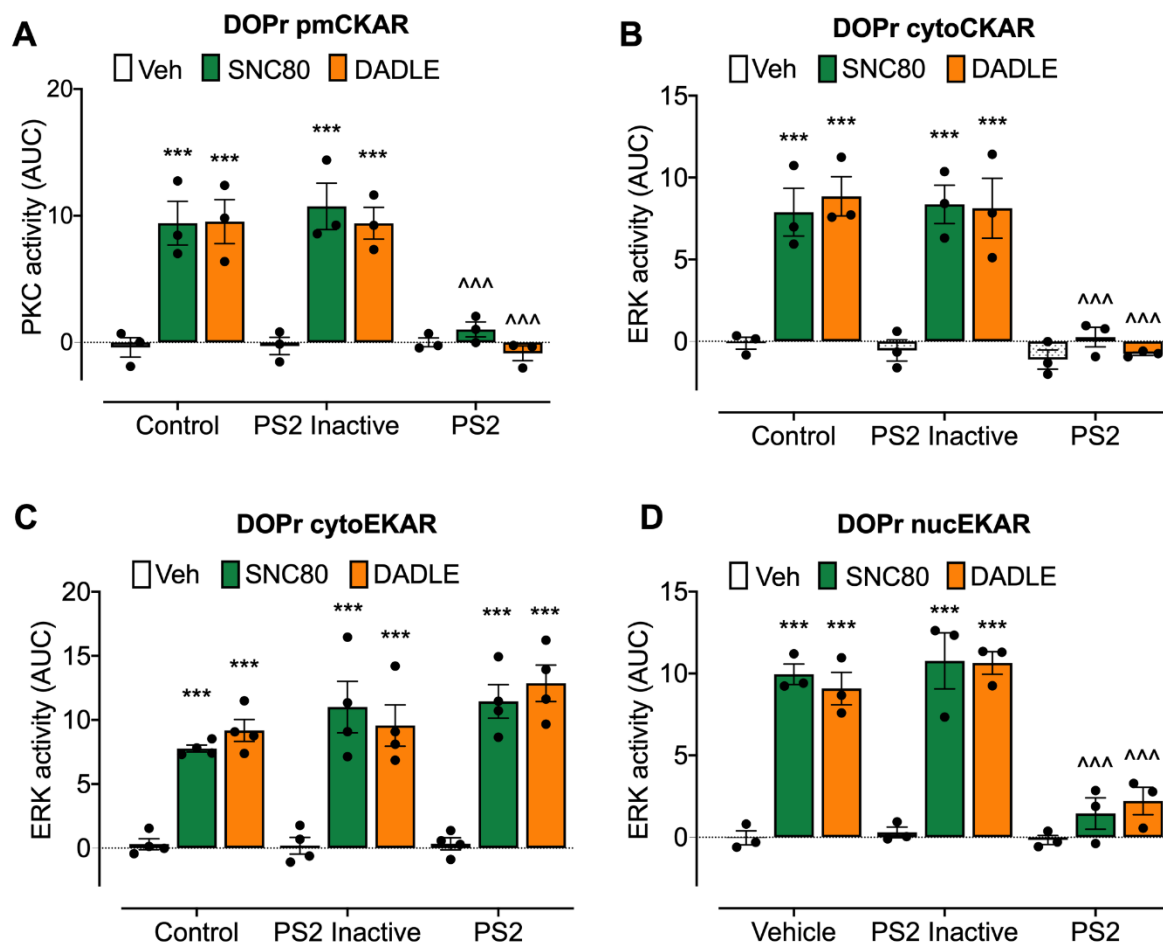


Fig. S3. Endosomal DOPr-mediated PKC and ERK signaling in subcellular compartments of HEK293 cells. FRET biosensors for plasma membrane and cytosolic PKC (pmCKAR, cytoCKAR) or cytosolic and nuclear ERK (cytoEKAR, nucEKAR) were coexpressed with DOPr in HEK293 cells. Cells were pretreated with vehicle, PS2 inactive or PS2. **A.** Plasma membrane PKC activity. **B.** Cytosolic PKC activity. **C.** Cytosolic ERK activity. **D.** Nuclear ERK activity. Integrated responses over 20 min (area under the curve, AUC). Data points show results of independent experiments. N=3 independent experiments (mean±SEM). *** $P < 0.001$ ligand to vehicle; ^^ $P < 0.001$ inhibitors to control; 2-way ANOVA, Tukey's test.

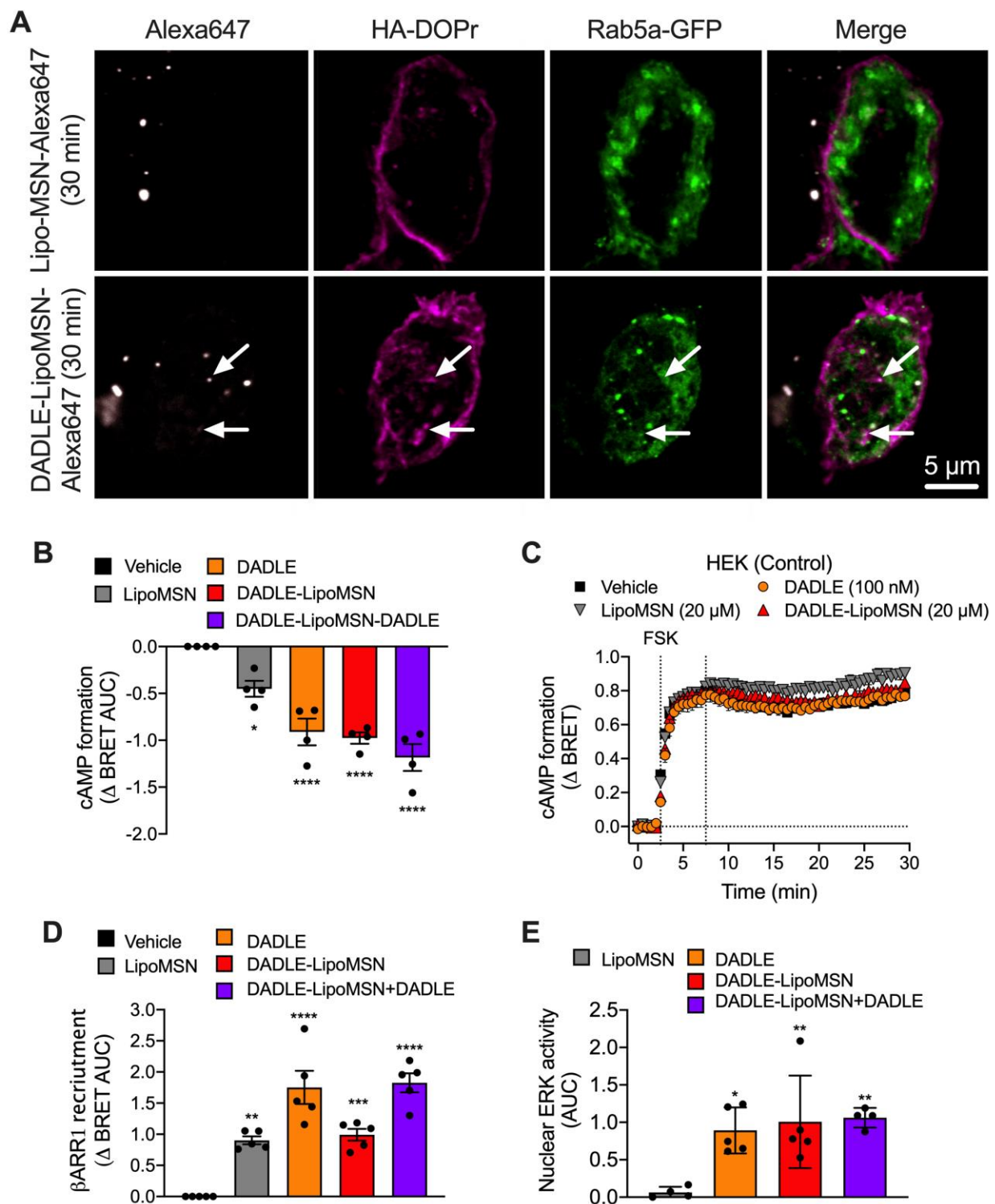


Fig. S4. Uptake and signaling of DADLE nanoparticles in HEK293 cells. **A.** Uptake of DADLE-LipoMSN-DADLE-Alexa647 into HEK-HA-DOPr cells after 30 min. Representative images, N=4 experiments. **B, C.** Effects of DADLE (100 nM), DADLE-LipoMSN (20 μ M) and DADLE-LipoMSN-DADLE (20 μ M) on forskolin (FSK, 10 μ M)-stimulated cAMP formation in

HEK-DOPr cells (**B**, AUC, area under curve) and HEK293 control cells (**C**). Effects of DADLE (100 nM), DADLE-LipoMSN (20 μ M) and DADLE-LipoMSN-DADLE (20 μ M) on β ARR1 recruitment (**C**) and activation of nuclear ERK (**D**) in HEK-DOPr cells. Data points show results of independent experiments. N=4 (**B**), N=5 (**C-E**) (independent experiments (mean \pm SEM). * P <0.05, ** P <0.01, *** P <0.001, **** P <0.0001, 1-way ANOVA, Tukey's test.

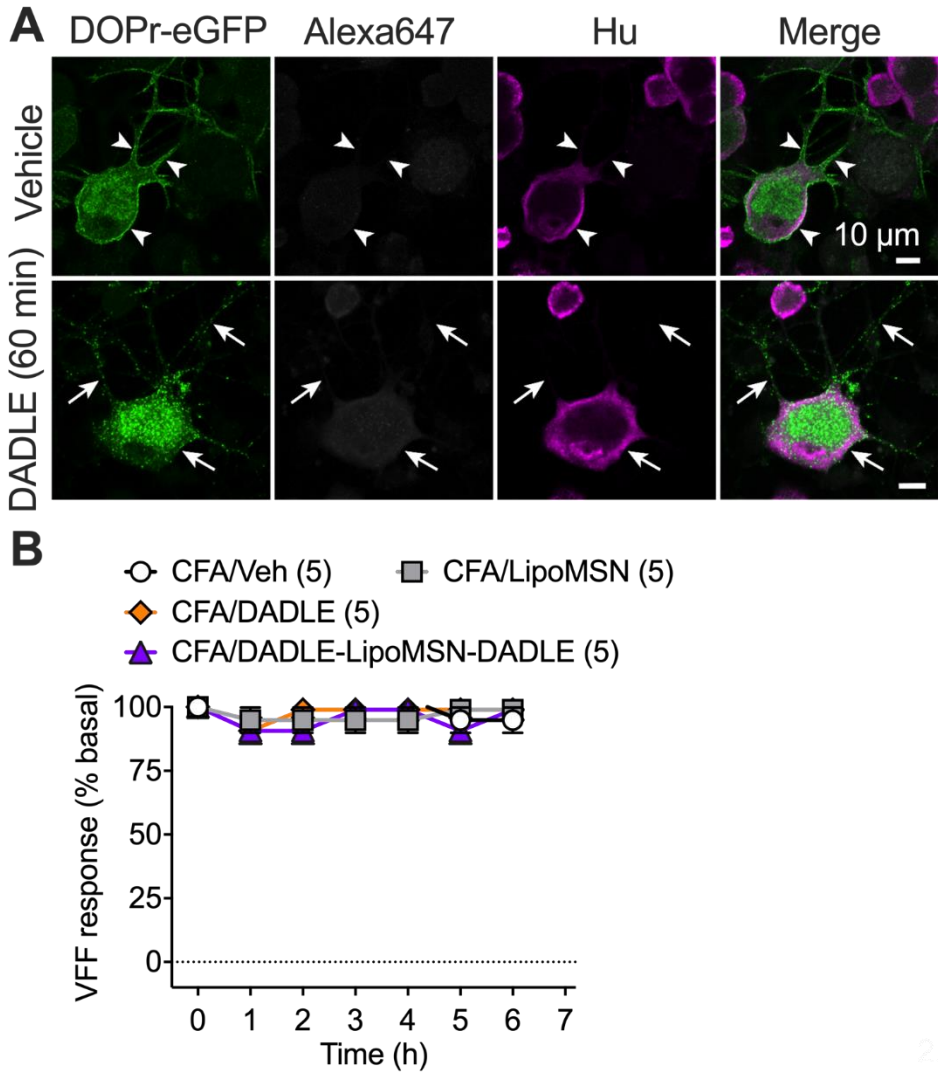


Fig. S5. Agonist-evoked endocytosis of DOPr-eGFP in nociceptors and assessment of nociception in mice. **A.** Localization of DOPr-eGFP in DRG neurons from DOPr-eGFP knockin mice after incubation with DADLE (1 μ M) or vehicle for 60 min. Representative images of N=4 independent experiments. Nanoparticles were omitted from this experiment; thus, there is no Alexa647 signal. **B.** Contralateral paw withdrawal responses in mice. DADLE, DADLE-LipoMSN-DADLE (both 100 nM DADLE), LipoMSN or vehicle (Veh) was injected intrathecally at 48 h after intraplantar CFA. N=5 mice per group (mean \pm SEM).

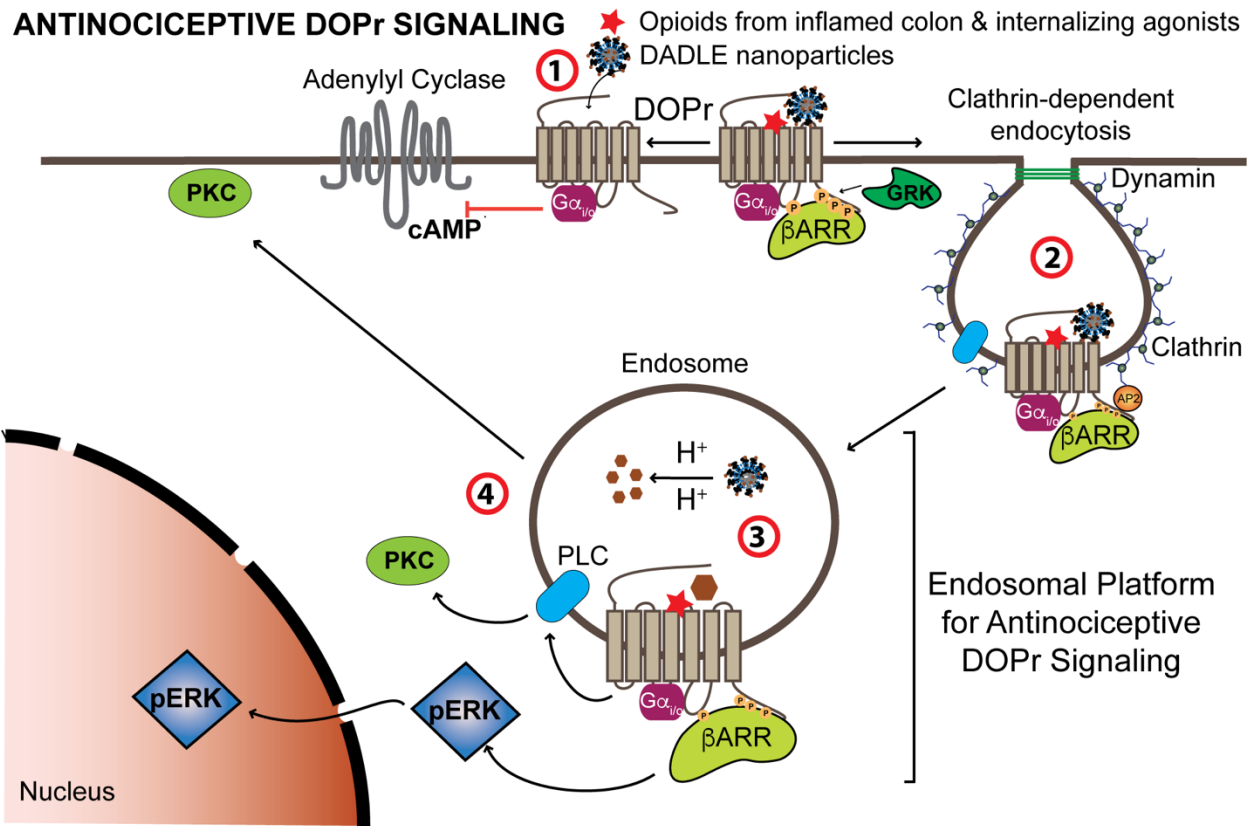


Fig. S6. Agonist stimulated trafficking of DOPr mediates compartmentalized signaling and antinociception. 1. Opioids from the inflamed colon, internalizing agonists (DADLE, SNC80), and DADLE-LipoMSN-DADLE activate plasma membrane DOPr, which couples to activation of $G\alpha_{i/o}$ and recruits β ARRs. 2. DOPr undergoes clathrin- and dynamin-mediated endocytosis. Within endosomes, DOPr continues to signal. 3. When activated by opioids from the inflamed colon, internalizing agonists (DADLE, SNC80), and DADLE-LipoMSN-DADLE, endosomal DOPr generates sustained signals. 4. Endosomal DOPr activates plasma membrane and cytosolic PKC in addition to cytosolic and nuclear ERK. These signals mediate the antinociceptive actions of endosomal DOPr.

Table S1. Clinical score of patients with UC

Diagnosis	Chronicity of symptoms	Endoscopy score severity	Age (y)	Sex	Treatment
Ulcerative colitis	> 3 months	Mayo 1	49	M	5-ASA
Ulcerative proctitis	> 3 months	Mayo 2	59	F	5-ASA
Ulcerative colitis	> 3 months	Mayo 1-2	62	M	5-ASA

MAYO score 0-3. 5-ASA, 5-aminosalicylic acid.

Table S2. Statistical tests

Experiment	Statistical tests
Excitability of DRG nociceptors	2-way ANOVA, Tukey's test
Excitability of colonic nociceptors	2-way ANOVA, Tukey's test, Sidak's test
BRET assays	1- or 2-way ANOVA, Tukey's test
FRET assays	1- or 2-way ANOVA, Tukey's test
Nanoparticle uptake	T-test, Holm-Sidak correction 1-way ANOVA, Tukey's test
Nociceptive behavior	2-way ANOVA, Tukey's test

Movie S1. Uptake of DADLE-LipoMSN-Alexa647 into HEK-DOPr cells. HEK-HA-DOPr cells expressing Rab5a-GFP were incubated with DADLE-LipoMSN-Alexa647 (20 μ M DADLE). Live cells were imaged by confocal microscopy.

Movie S2. Lack of uptake of LipoMSN-Alexa647 into HEK-DOPr cells. HEK-HA-DOPr cells expressing Rab5a-GFP were incubated with LipoMSN-Alexa647 (control). Live cells were imaged by confocal microscopy.

References

1. G. Scherrer *et al.*, Knockin mice expressing fluorescent delta-opioid receptors uncover G protein-coupled receptor dynamics in vivo. *Proc Natl Acad Sci U S A* **103**, 9691-9696 (2006).
2. E. E. Valdez-Morales *et al.*, Sensitization of peripheral sensory nerves by mediators from colonic biopsies of diarrhea-predominant irritable bowel syndrome patients: a role for PAR2. *Am J Gastroenterol* **108**, 1634-1643 (2013).
3. N. N. Jimenez-Vargas *et al.*, Protease-activated receptor-2 in endosomes signals persistent pain of irritable bowel syndrome. *Proc Natl Acad Sci U S A* **115**, E7438-E7447 (2018).
4. R. Guerrero-Alba *et al.*, Co-expression of mu and delta opioid receptors by mouse colonic nociceptors. *Br J Pharmacol* **175**, 2622-2634 (2018).

5. E. Valdez-Morales *et al.*, Release of endogenous opioids during a chronic IBD model suppresses the excitability of colonic DRG neurons. *Neurogastroenterol Motil* **25**, 39-46 e34 (2013).
6. S. M. Brierley, R. C. Jones, 3rd, G. F. Gebhart, L. A. Blackshaw, Splanchnic and pelvic mechanosensory afferents signal different qualities of colonic stimuli in mice. *Gastroenterology* **127**, 166-178 (2004).
7. P. A. Hughes *et al.*, Post-inflammatory colonic afferent sensitisation: different subtypes, different pathways and different time courses. *Gut* **58**, 1333-1341 (2009).
8. N. Audet *et al.*, Differential association of receptor-Gbetagamma complexes with beta-arrestin2 determines recycling bias and potential for tolerance of delta opioid receptor agonists. *J Neurosci* **32**, 4827-4840 (2012).
9. J. S. Herskovits, C. C. Burgess, R. A. Obar, R. B. Vallee, Effects of mutant rat dynamin on endocytosis. *J Cell Biol* **122**, 565-578 (1993).
10. C. Gales *et al.*, Probing the activation-promoted structural rearrangements in preassembled receptor-G protein complexes. *Nat Struct Mol Biol* **13**, 778-786 (2006).
11. T. H. Lan, Q. Liu, C. Li, G. Wu, N. A. Lambert, Sensitive and high resolution localization and tracking of membrane proteins in live cells with BRET. *Traffic* **13**, 1450-1456 (2012).
12. Q. Wan *et al.*, Mini G protein probes for active G protein-coupled receptors (GPCRs) in live cells. *J Biol Chem* **293**, 7466-7473 (2018).
13. Y. Namkung *et al.*, Monitoring G protein-coupled receptor and beta-arrestin trafficking in live cells using enhanced bystander BRET. *Nat Commun* **7**, 12178 (2016).
14. C. D. Harvey *et al.*, A genetically encoded fluorescent sensor of ERK activity. *Proc Natl Acad Sci U S A* **105**, 19264-19269 (2008).
15. L. L. Gallegos, M. T. Kunkel, A. C. Newton, Targeting protein kinase C activity reporter to discrete intracellular regions reveals spatiotemporal differences in agonist-dependent signaling. *J Biol Chem* **281**, 30947-30956 (2006).
16. D. D. Jensen *et al.*, Endothelin-converting enzyme 1 and beta-arrestins exert spatiotemporal control of substance P-induced inflammatory signals. *J Biol Chem* **289**, 20283-20294 (2014).
17. D. D. Jensen *et al.*, Neurokinin 1 receptor signaling in endosomes mediates sustained nociception and is a viable therapeutic target for prolonged pain relief. *Sci Transl Med* **9**, eaal3447 (2017).
18. R. Nehme *et al.*, Mini-G proteins: Novel tools for studying GPCRs in their active conformation. *PLoS One* **12**, e0175642 (2017).
19. P. Donthamsetti, J. R. Quejada, J. A. Javitch, V. V. Gurevich, N. A. Lambert, Using Bioluminescence Resonance Energy Transfer (BRET) to Characterize Agonist-Induced Arrestin Recruitment to Modified and Unmodified G Protein-Coupled Receptors. *Curr Protoc Pharmacol* **70**, 2 14 11-12 14 14 (2015).
20. M. L. Halls, D. P. Poole, A. M. Ellisdon, C. J. Nowell, M. Canals, Detection and Quantification of Intracellular Signaling Using FRET-Based Biosensors and High Content Imaging. *Methods Mol Biol* **1335**, 131-161 (2015).
21. D. Shao *et al.*, Bioinspired Diselenide-Bridged Mesoporous Silica Nanoparticles for Dual-Responsive Protein Delivery. *Adv Mater* 10.1002/adma.201801198, e1801198 (2018).

22. M. Wang *et al.*, Efficient delivery of genome-editing proteins using bioreducible lipid nanoparticles. *Proc Natl Acad Sci U S A* **113**, 2868-2873 (2016).
23. J. N. Moreira, T. Ishida, R. Gaspar, T. M. Allen, Use of the post-insertion technique to insert peptide ligands into pre-formed stealth liposomes with retention of binding activity and cytotoxicity. *Pharm Res* **19**, 265-269 (2002).
24. P. D. Ramírez-García *et al.*, A pH-responsive nanoparticle targets the neurokinin 1 receptor in endosomes to prevent chronic pain. *Nature Nanotechnology* 10.1038/s41565-019-0568-x (2019).